such a case should be lower than the barrier for distances that are closer to equilibrium (2.8–2.9 Å).

A persistent question, the mode of activation of Ser to become a powerful nucleophile, thus may be viewed in a new light as a result of these simulations. The effect of protein-mediated close contact of donor and acceptor may be one of the factors that increases the speed and efficiency of this enzymatic reaction. Quantum chemical methods should be employed to elucidate the problem. These calculations are now in progress in this laboratory.

Acknowledgment. We thank Mgr Antoni Łączkowski for help in displaying some of the statistical data. Financial support has been provided by the National Science Foundation (DMB - 8517286), Robert A. Welch Foundation (A-328) and the Texas Agriculture Experiment Station. Computational resources were provided by the Pittsburgh Supercomputing Center and Associate Provost for Computing, Dr. John Dinkel. M.G. wishes to acknowledge travel support from the Ministry of Science and Higher Education (Poland) within the project C.P.B.P. 01.06.

Supplementary Material Available: Minimized sterodrawing of the active-site region of PPE (Figure 1b), time evolution of selected distances between the side chain of Ser-195 and His-214 (Figure 2a) and Ser-214 and nVal-3 (Figure 2b) in MD simulation of a Michaelis complex, and time evolution of a H-bonding network in the active site of a Michaelis with $\Phi = 55°$ (Figure 4b) (4 pages). Ordering information is given on any current masthead page.

(44) Lesyng, B., private communication.

Sterically Encumbered Functional Groups: An Investigation of Endo versus Exo Phosphoryl Complexation Using ^1H and ^{31}P NMR

Bernard P. Friedrichsen, Douglas R. Powell,† and Howard W. Whitlock*

Contribution from the Samuel M. McElvain Laboratories of Organic Chemistry, Chemistry Department, University of Wisconsin—Madison, Madison, Wisconsin 53706.
Received May 21, 1990. Revised Manuscript Received July 23, 1990

Abstract: The synthesis of phosphine oxide bifunctional macrocycles **1–4** is reported. Additionally, the X-ray crystal structures for exo–exo diyne **1** and endo–exo hosts **2** and **4** are presented. Assignment of the two phosphorus signals in the ^{31}P NMR spectra of **2** and **4** and the aromatic proton signals in the ^1H NMR spectra of **2** and **4** is reported. The complexation behavior of macrocycles **1–4** and precyclophane **8** with a variety of neutral organic guests and Ph_2SnCl_2 is investigated by using ^1H and ^{31}P NMR as investigative instrumental probes. Initial endo complexation is the preferred mechanism in the 1:2 complexation of **2** with guests, while initial exo complexation is preferred for the complexation of **4** with guests. **2** forms 1:2 complexes with pentafluorophenol, 2,6-dimethyl-4-nitrophenol, and acetic acid via initial exo complexation. Association constants determined from these experiments reveal that the exo phosphoryl binding site in **4** is higher than those in the other reported phosphine oxides. An X-ray crystal structure of the 1:1 complex of **4** with diphenyltin dichloride was obtained to explore this anomaly, and it is reported.

Introduction

This paper describes the synthesis and complexation behavior of phosphine oxide bifunctional macrocycles **1–4** (Figure 1).[1] The design of host molecules capable of binding neutral organic guests is an area of rapidly expanding interest.[2] Cram,[3] Lehn,[4] Vögtle,[5] Diederich,[6] and others have made significant advances in the field of host–guest complexation.[7] Some of our past and continuing research has led to the construction of large preorganized macrocyclic cavities bearing concave functionalities.[8] Most of these have utilized naphthalenes and diyne bridges as their basic structural units while pyridines have served as the hydrogen-bond accepting sites. We were interested in expanding our arsenal of complexation functionality as well as our general structural framework. In 1985 Breslow et al. communicated the synthesis of an exo(C-Me)–exo(C-Me) host.[9] We were interested in the anatomical structure of this species since it closely resembles our own macrocycles with its diyne bridges and well-defined three-dimensional cavity. Phosphine oxides have been recognized as strong hydrogen-bond acceptors,[10] and we contemplated using these as our loci complexation. Etter has recently reported the successful cocrystallization of various hydrogen donors with triphenylphosphine oxide.[11] Most of the literature regarding phosphorus-containing macrocycles has focused on the development of macrocyclic phosphines and phosphites as ligands for

† X-ray crystallographer for the Chemistry Department at the University of Wisconsin—Madison.

(1) Friedrichsen, B. P.; Whitlock, H. W. *J. Am. Chem. Soc.* **1989**, *111*, 9132.
(2) For an excellent review, see: Diederich, F. *Angew. Chem., Int. Ed. Engl.* **1988**, *27*, 362–386.
(3) (a) Tucker, A. J.; Knobler, C. B.; Trueblood, K. N.; Cram, D. J. *J. Am. Chem. Soc.* **1989**, *111*, 3688. (b) Paek, K. S.; Cram, D. J. *Bull. Kor. Chem. Soc.* **1989**, *10*, 568. (c) Sherman, J. C.; Cram, D. J. *J. Am. Chem. Soc.* **1989**, *111*, 4257.
(4) (a) Fages, F.; Desvergne, J. P.; Kotzybahibert, F.; Lehn, J. M.; Marsau, P.; Albrechtgary, A. M.; Bouaslaurent, H.; Aljoubbeh, M. *J. Am. Chem. Soc.* **1989**, *111*, 8672. (b) Hosseini, M. W.; Lehn, J. M.; Comarmand, J. *Helv. Chim. Acta* **1989**, *72*, 1066. (c) Hosseini, M. W.; Kintzinger, J. P.; Lehn, J. M.; Zahidi, A. *Helv. Chim. Acta* **1989**, *72*, 1078.
(5) (a) Wallon, A.; Peter-Katalinic, J.; Werner, W. M.; Vögtle, F. *Chem. Ber.* **1990**, *123*, 375. (b) Peter-Katalinic, J.; Ebmeyer, F.; Seel, C.; Vögtle, F. *Chem. Ber.* **1989**, *122*, 2391. (c) Ebmeyer, F.; Vögtle, F. *Chem. Ber.* **1989**, *122*, 1725.
(6) Seward, E. M.; Hopkins, R. B.; Sauerer, W.; Tam, S. W.; Diederich, F. *J. Am. Chem. Soc.* **1990**, *112*, 1783. (b) Hester, M. R.; Uyecki, M. A.; Diederich, F. *Isr. J. Chem.* **1989**, *29*, 201. (c) Diederich, F.; Cutter, H. D. *J. Am. Chem. Soc.* **1989**, *111*, 8438.
(7) (a) Breslow, R.; Greenspoon, N.; Guo, T.; Zarzycki, R. *J. Am. Chem. Soc.* **1989**, *111*, 8296. (b) Petti, M. A.; Sheppod, T. J.; Dougherty, D. A. *Tetrahedron Lett.* **1986**, *27*, 5563. (c) Canceill, J.; Lacombe, L.; Collet, A. *J. Am. Chem. Soc.* **1986**, *108*, 4230. (d) Williams, K.; Askew, B.; Ballester, P.; Buhr, C.; Jeong K. S.; Jones, S.; Rebek, J., Jr. *J. Am. Chem. Soc.* **1989**, *111*, 1090.

0002-7863/90/1512-8931$02.50/0

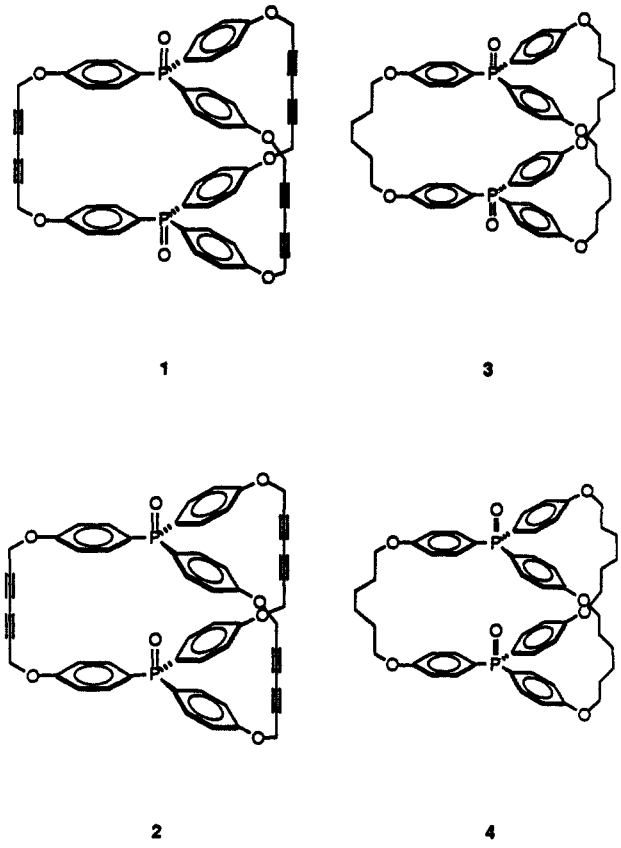

Figure 1. Representations of the four phosphine oxide bifunctional macrocycles.

transition metals.[12] Several phosphoryl-containing macrocycles have been reported.[13] The first X-ray structure of a synthetic phosphoryl-containing macrocycle was reported by Drager in 1974.[14] Cram has investigated the binding properties of macrocyclic ethers containing phosphoryl and *N*-oxide groups with alkali metal salts.[15] We have incorporated the phosphine oxide functionality into a host by using dioxadiyne bridges which we have previously shown to be an efficient means of designing and constructing rigid cavities[8] to synthesize tribridged phosphoryl-bearing hosts **1** and **2**.[1] Reduction of the diyne bridges provided the saturated bridge species **3** and **4**. Together, these four hosts have allowed us to explore the complexation of phosphine oxides within molecular cavities. In an effort to further explore the binding properties of macrocycles **1–4** and precyclophane **8** with various phenolic guests, we carried out titration experiments

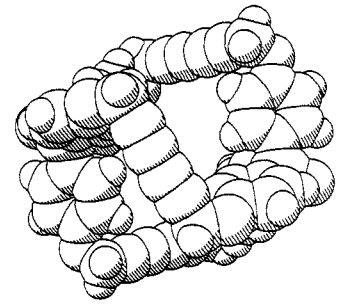

Figure 2. Space-filling representation of **1** generated by SHELXTL PLUS, based on X-ray data collected at −150 °C. Solvent molecules are excluded from the structure. The final *R* value after refinement was 0.108. The P–P distance is 10.85 Å.

Scheme I

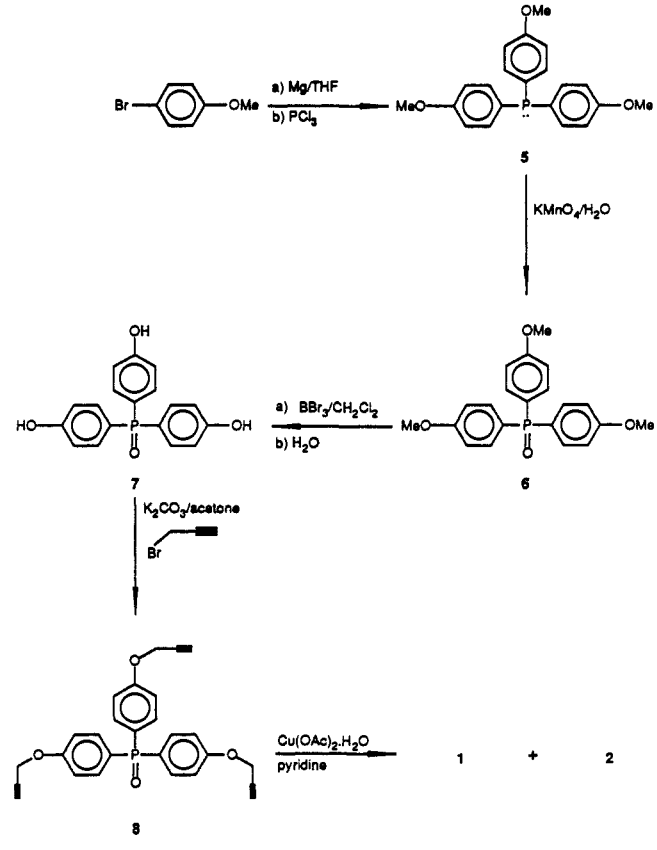

utilizing ^{31}P and ^{1}H NMR as investigative instrumental probes. This necessitated the assignment of the aromatic ^{1}H NMR signals as well as the two ^{31}P NMR signals of endo–exo hosts **2** and **4**. We were able to obtain X-ray crystallographic data on **1**, **2**, **4**, and the 1:1 complex of **4** with diphenyltin dichloride.

Synthesis

The synthetic route utilized in the construction of the isomeric diyne-bridged phosphine oxide bifunctional macrocycles **1** and **2** is illustrated in Scheme I. Tris(4-methoxyphenyl)phosphine (**5**) was prepared in 56% yield after recrystallization by reaction of phosphorus trichloride with the Grignard reagent prepared from *p*-bromoanisole as reported by Mann and Chaplin.[16] Oxidation of the phosphine **5** by reaction with potassium permanganate in water afforded **6** in 86% yield. Deprotection of the previously reported tris(4-methoxyphenyl)phosphine oxide (**6**)[17] was performed by using boron tribromide in methylene chloride, affording

(8) (a) Sheridan, R. E.; Whitlock, H. W., Jr. *J. Am. Chem. Soc.* **1988**, *110*, 4071. (b) Sheridan, R. E.; Whitlock, H. W., Jr. *J. Am. Chem. Soc.* **1986**, *108*, 7120. (c) Whitlock, B. J.; Whitlock, H. W., Jr. *J. Am. Chem. Soc.* **1985**, *107*, 1325. (d) Miller, S. P.; Whitlock, H. W., Jr. *J. Am. Chem. Soc.* **1984**, *106*, 1492.

(9) O'Krongly, D.; Denmeade, S. R.; Chiang, M. Y.; Breslow, R. *J. Am. Chem. Soc.* **1985**, *107*, 5544.

(10) (a) Toda, F.; Mori, K.; Stein, Z.; Goldberg, I. *J. Org. Chem.* **1988**, *53*, 308. (b) Arnett, E. M.; Mitchell, E. J.; Murty, T. S. S. R.; Gorrie, T. M.; Schleyer, P. v. R. *J. Am. Chem. Soc.* **1970**, *92*, 2365. (c) Arnett, E. M.; Mitchell, E. J.; Murty, T. S. S. R. *J. Am. Chem. Soc.* **1974**, *96*, 3875. (d) Hadzi, D.; Smerkolj, R. *J. Chem. Soc., Faraday Trans. 1* **1976**, 1188.

(11) Etter, M. C.; Baures, P. W. *J. Am. Chem. Soc.* **1988**, *110*, 639.

(12) For an excellent review, see: Tsetkov, E. N.; Bovin, A. N.; Syundyukova, V. K. *Russ. Chem. Rev.* **1988**, *57*, 1353–1402.

(13) (a) Bolm, C.; Sharpless, K. B. *Tetrahedron Lett.* **1988**, *29*, 5101. (b) Muller, E.; Burgi, H. B. *Helv. Chim. Acta* **1987**, *70*, 1063. (c) Chan, T. H.; Ong, B. S. *J. Org. Chem.* **1974**, *39*, 1748. (d) Kirasanov, A. V.; Kudrya, T. N.; Balina, L. V.; Shtepanek, A. S. *Dokl. Akad. Nauk. SSSR* **1979**, *247*, 613. (e) Christol, H. J.; Fallouh, F.; Hullot, P. *Tetrahedron Lett.* **1979**, *28*, 2591. (f) Yatsimirskii, K. B.; Kabachnik, M. I.; Sinyavskaya, E. I.; Medved, T. Ya.; Polikarpov, Yu. M.; Bodvin, G. V. Russ. *J. Inorg. Chem.* **1980**, *25*, 1302.

(14) Drager, *Chem. Ber.* **1974**, *107*, 3246.

(15) Kaplan, L. J.; Weisman, G. R.; Cram, D. J. *J. Org. Chem.* **1979**, *44*, 2226.

(16) Mann, F. G.; Chaplin, E. J. *J. Chem. Soc.* **1937**, 527.

(17) Bailey, W. J.; Buckler, S. A.; Marktscheffel, F. *J. Org. Chem.* **1960**, *25*, 1996.

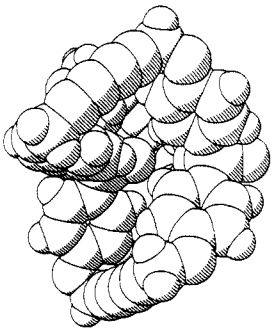

Figure 3. Space-filling representation of **2** generated by SHELXTL PLUS, based on X-ray collected at −165 °C. Solvent molecules are excluded from the structure. The final *R* value after refinement was 0.114. The O_{endo}–P_{exo} distance is 4.20 Å.

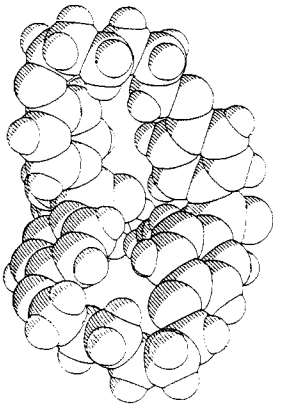

Figure 4. Space-filling representation of **4** generated by SHELXTL PLUS, based on X-ray data collected at −100 °C. Ethyl acetate and water are excluded from the structure. The final *R* value after refinement was 0.060. The O_{endo}–P_{exo} distance is 4.68 Å.

the known tris(4-hydroxyphenyl)phosphine oxide (**7**) in 97% yield after recrystallization.[17] Alkylation of **7** carried out with potassium carbonate and propargyl bromide in acetone afforded the precyclophane (**8**) in 78% yield. We reasoned that the dimeric coupling of **8** would proved exo–exo diyne **1** and endo–exo diyne **2** since CPK models of the isomers suggested that no severe steric interactions were present. Treatment of **8** in pyridine (0.008M) at 60 °C with $Cu(OAc)_2 \cdot H_2O$ for 2 h provided **1** and **2** in 14% and 7% yields, respectively, after purification and recrystallization. Hydrogenation of **1** was carried out in DMF with use of 5% palladium on calcium carbonate producing **3** in 47% yield after recrystallization. Similarly, hydrogenation of **2** afforded **4** in 53% yield after crystallization.

X-ray Structures

Monoclinic crystals of **1** obtained from chloroform were suitable for an X-ray structure determination. The space-filling representation (Figure 2), excluding solvent, confirms the exo orientation of both phosphine oxides. The P–P distance is 10.85 Å and provides a good measure of the cavity dimension.[1] The helical nature of **1** is evident upon examination of the crystal structure. Chloroform resides within the cavity, but is disordered.

Triclinic crystals of **2** were obtained from anisole upon slow evaporation of the solvent. Both the endo–exo orientation of the phosphoryls and the helical nature of the species are apparent upon examination of the structure, excluding solvent (Figure 3). The P–P distance is 5.68 Å, and the endo-oxygen–exo-phosphorus (O_{endo}–P_{exo}) distance is 4.20 Å. The O_{endo}–P_{exo} distance is a better measure of cavity dimension for the endo–exo species. The cavity does not contain solvent.

Triclinic crystals of **4** suitable for X-ray analysis were grown from wet ethyl acetate.[1] The molecule does not exhibit the helical nature to the same degree (Figure 4) as seen in the two diyne hosts (**1** and **2**). Water in the crystal structure was observed to reside in either of two locations: Both show hydrogen bonding to the

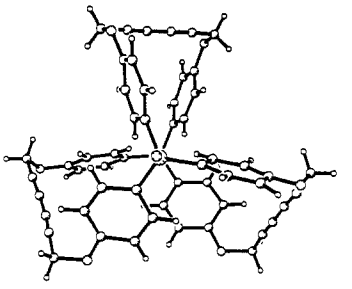

Figure 5. The pseudo-Newman X-ray crystal structure projection of **1** viewed down the O–P bond.

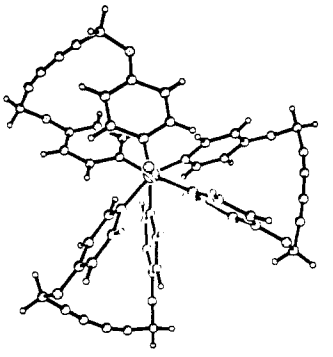

Figure 6. The pseudo-Newman X-ray crystal structure projection of **2** viewed down the exo phosphoryl O–P bond.

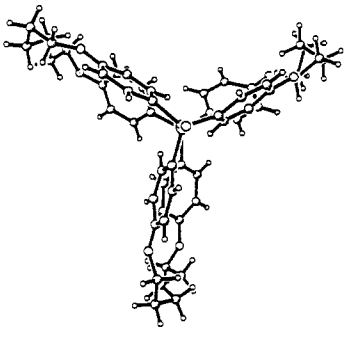

Figure 7. The pseudo-Newman X-ray crystal structure projection of **4** viewed down the exo phosphoryl O–P bond.

exo oxygen (O_{exo}). The P–P distance is 6.15 Å, and the O_{endo}–P_{exo} distance is 4.68 Å.

The pseudo-Newman projections of **1**, **2**, and **4** are shown in Figures 5, 6 and 7, respectively, looking down the exo phosphoryl O=P bond. The projections of diyne hosts **1** and **2** show an almost completely "staggered" conformation in contrast to the projection of the saturated bridge host (**4**) which exhibits the almost completely "eclipsed" conformation. The difference in the conformations of the diyne hosts and the saturated bridge host is attributed to rigidity in the diyne bridges.

Assignment of ^{31}P and ^{1}H NMR signals

Assignment of ^{31}P NMR Signals. Assignment of the ^{31}P NMR signals was imperative for the two endo–exo species (**2** and **4**). Two signals were observed in each of the ^{31}P NMR spectra of endo–exo hosts **2** and **4**. We designated the downfield peak as P_1 (**2**, 25.39 ppm; **4**, 28.40 ppm) and the upfield peak as P_2 (**2**, 25.09 ppm; **4**, 24.81 ppm). We speculated that a sterically hindered guest would complex with a high degree of regioselectively to the exo phosphoryl sites in the two endo–exo species since the endo sites are sterically encumbered. We predicted that the change in chemical shift ($\Delta\delta$) of the exo phosphoryl phosphorus (P_{exo}) should be significnatly greater than the $\Delta\delta$ of the endo phosphoryl phosphorus (P_{endo}) upon addition of a suitably hindered guest. Diphenyltin dichloride is known to form 1:1 complexes with triphenylphosphine oxide in chloroform and is a rather bulky Lewis

Table I. Experimental Data Determined from Titration of **8**, **2**, and **4** with Diphenyltin Dichloride in $CDCl_3$ at 25 °C by Using ^{31}P NMR

experimentally determined data	phosphine oxide 8	2	4
K_a, L/M[a]	138	243	732
δ P_{exo}, ppm[b]	NA[c]	25.39	28.40
$\Delta\delta$ P_{exo}, ppm[c]	NA[c]	+7.84	+7.14
δ P_{endo}, ppm[b]	NA[c]	25.09	24.81
$\Delta\delta$ P_{endo}, ppm[c]	NA[c]	+0.27	+0.12
δ P, ppm[b]	27.50	NA[c]	NA[c]
$\Delta\delta$ P, ppm[d]	+5.63	NA[c]	NA[c]

[a] Association constants were determined, assuming 1:1 complexation, with use of Simplex. [b] The chemical shifts of the species in $CDCl_3$ with PPh_3 in THF as an external reference (δ = -6.00 ppm). [c] The change in chemical shift after addition of 10 equiv of Ph_2SnCl_2: [H] = 0.005 M, [G] = 0.05 M. [d] The change in chemical shift after addition of 5 equiv of Ph_2SnCl_2: [H] = 0.010 M, [G] = 0.05 M. [e] The value is not applicable for this species.

Table II. Assigned Aromatic ^1H NMR Signals of Phosphine Oxide Macrocycles **1**-**4** in $CDCl_3$ with TMS as an Internal Reference

type of aromatic proton	phosphine oxide hosts: δ, ppm 1	2	3	4
ortho to P_{exo}[a]	7.67	8.06	7.50	7.86
ortho to P_{endo}[b]	NA[c]	7.63	NA[c]	7.51
meta to P_{exo}[a]	7.07	7.08	6.84	6.81
meta to P_{endo}[b]	NA[c]	7.08	NA[c]	6.94

[a] The protons ortho and meta to the exo phosphoryl functionality. [b] The protons ortho and meta to the endo phosphoryl functionality. [c] The value is not applicable for this species.

acid.[18] Therefore, we chose this Lewis acid as our guest for assigning ^{31}P NMR signals.

Titration of a solution of precyclophane **8** in chloroform (0.02 M) with a solution of Ph_2SnCl_2 in chloroform (0.10 M) at room temperature resulted in a large downfield shift ($\Delta\delta$ = +5.63 ppm) of the ^{31}P signal upon addition of 5 equiv of the tin reagent. Titration of a solution of **2** in chloroform (0.01 M) with a solution of Ph_2SnCl_2 in chloroform (0.101M) resulted in downfield shifts for both P signals. After addition of 10 equiv of guest, the chemical shift of P_1 was 33.23 ppm ($\Delta\delta$ = +7.84 ppm), and the chemical shift of P_2 was 25.36 ppm ($\Delta\delta$ = +0.27 ppm). Therefore, P_1 is the P_{exo} signal, and P_2 is the P_{endo} signal. Titration of **4** using the same initial concentrations of host and guest as were used in the study of **2** gave similar results. After addition of 10 equiv of guest, the chemical shift of P_1 was 35.54 ppm ($\Delta\delta$ = +7.14 ppm), and the chemical shift of P_2 was 24.93 ppm ($\Delta\delta$ = +0.12 ppm). Therefore, P_1 is the P_{exo} signal, and P_2 is the P_{endo} signal. The association constants (K_a's) assuming 1:1 complexation of the Ph_2SnCl_2 with **8**, **2**, and **4** were 138, 243, and 732 M^{-1}, respectively, as determined by a nonlinear least-squares curve-fitting program.[19] Yoder and co-workers have reported that the K_a for the 1:1 complex of triphenylphosphine oxide with Ph_2SnCl_2 in benzene at 25 °C is 295 M^{-1}.[20] A summary of these results is given in Table I.

Assignment of ^1H NMR Aromatic Signals. Since the aromatic protons in **2** and **4** are all coupled to phosphorus ($^3J_{PH}$ = 11.5 Hz, $^4J_{PH}$ = 2.5 Hz), and since the ^{31}P signals had all been assigned, ^{31}P-^1H 2D correlation NMR experiments allowed assignments of the aromatic protons. The 2D NMR ($CDCL_3$) of the endo-exo diyne **2** reveals that the signal of the proton ortho to P_{exo} occurs at 8.06 ppm while the proton ortho to P_{endo} occurs at 7.63 ppm. The meta protons exhibit accidental chemical shift equivalence

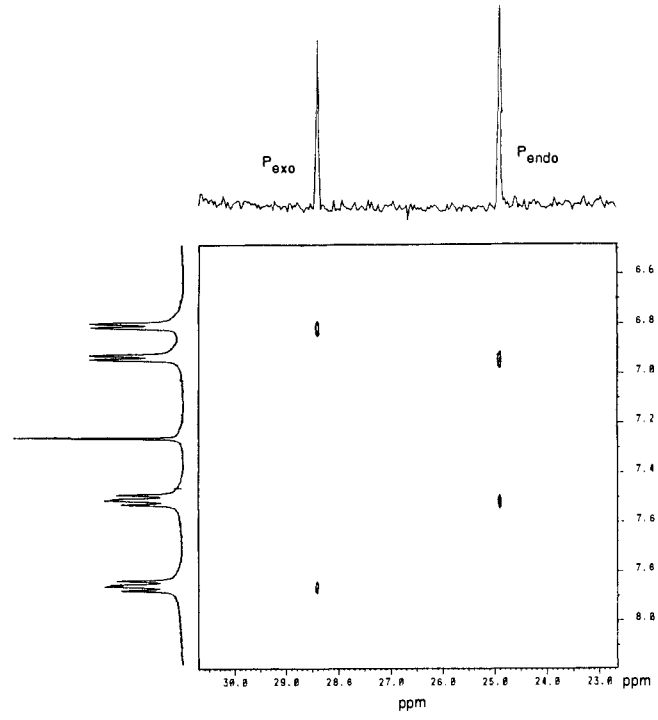

Figure 8. The ^{31}P-^1H 2D correlation NMR of **4** obtained on a Bruker AM-500 with $CDCl_3$ as the solvent. The signals corresponding to P_{exo} and P_{endo} are indicated.

Scheme II

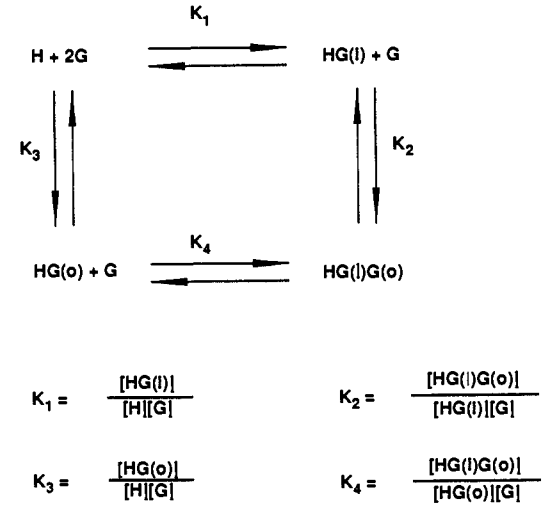

in **2**. The 2D NMR ($CDCl_3$) of **4** (Figure 8) reveals that the signals at 7.85 ppm and 6.81 ppm correspond to the protons ortho and meta to P_{exo}, respectively. The proton signals at 7.51 ppm and 6.94 ppm were assigned to the protons ortho and meta to P_{endo}, respectively. Table II summarizes the results from the 2D NMR experiments. In both **2** and **4** the protons ortho to P_{exo} are the furthest downfield. We propose that deshielding from the endo phosphoryl group is responsible for this phenomena.

Complexation Analysis

Since macrocyclic hosts **1**-**4** contain two phosphoryl sites, 1:2 complexation with phenols is expected. When the two phosphine oxide binding sites are identical, as is the case for the two exo-exo species **1** and **3**, only one mechanism exists for the formation of the 2:1 complex. When the two sites are identical and noninteracting, a 1:1 complexation model can be utilized if the concentration of the host is multiplied by two to give the effective concentration of phosphine oxide. We assume this is the case for **1** and **3** because the binding sites are relatively remote (**1**, P-P = 10.85 Å; O-O = 13.83 Å). The 1:1 complexation model is

(18) Mullins, P. *Can. J. Chem.* **1971**, *49*, 2719.
(19) A nonlinear least-squares-curve fitting program was written with use of the Simplex algorithm. The source (Turbo C) is available from the authors upon request. See: Noggle, J. H. *Physical Chemistry on a Microcomputer*; Little, Brown, and Co.: Boston, 1985; pp 145-165.
(20) Yoder, C. H.; Mokrynka, D.; Coley, S. M.; Otter, J. C.; Haines, R. E.; Grushaw, A.; Ansel, L. J.; Hovick, J. W.; Mikus, J.; Shermak, M. A.; Spencer, J. N. *Organometallics* **1987**, *6*, 1679.

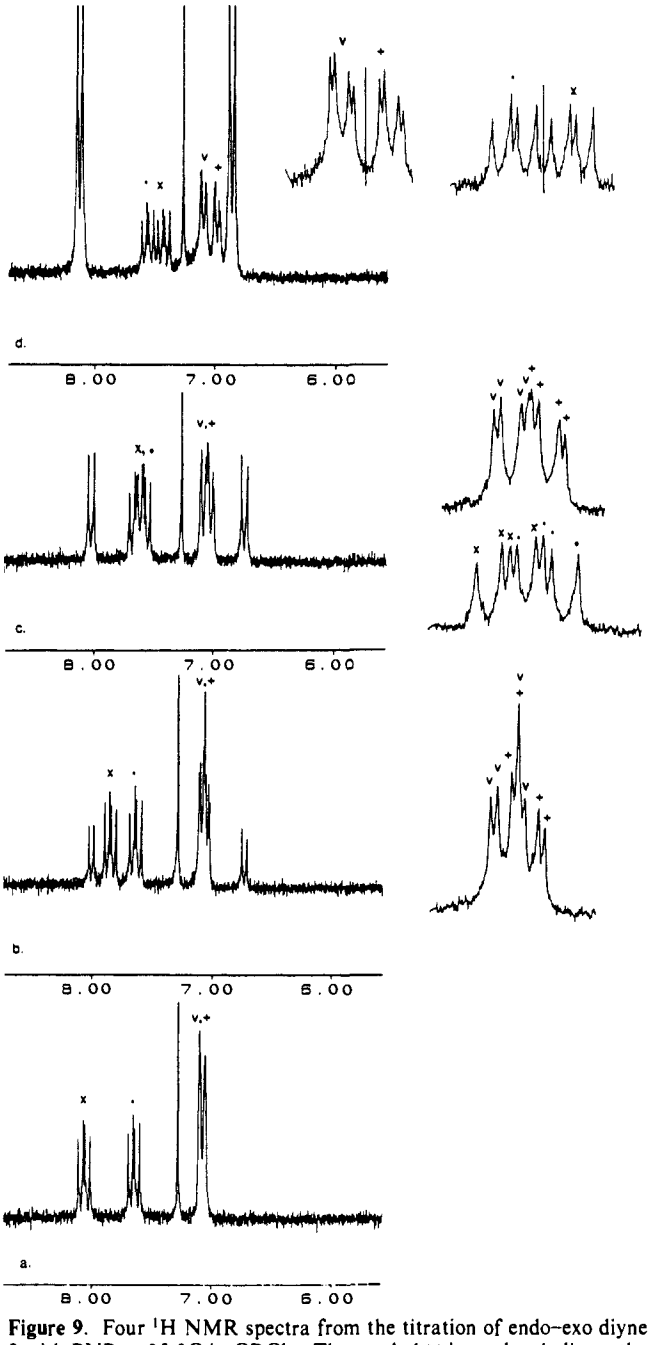

Figure 9. Four ^{1}H NMR spectra from the titration of endo–exo diyne **2** with PNP at 25 °C in $CDCl_3$. The symbol × is used to indicate the peaks corresponding to the protons ortho to P_{exo} while * designates those ortho to P_{endo}. + is used to indicate the protons meta to P_{exo} while v designates those meta to P_{endo} as determined by SPT: (a) The pure host in $CDCl_3$, [H] = 2.4×10^{-3} M; (b) 1 equiv of PNP added, [H] = 2.3×10^{-3} M, [PNP] = 2.3×10^{-3} M; (c) 2 equiv of PNP added, [H] = 2.25×10^{-3} M, [PNP] = 4.5×10^{-3} M; (d) 10 equiv of PNP added, [H] = 1.8×10^{-3} M, [PNP] = 1.8×10^{-2} M.

employed for studies with the precyclophane **8**. Two mechanisms may be proposed for the formation of 1:2 complexes if the binding sites are different (Scheme II). These involve initial complexation at either the endo or the exo binding site.

Titration Studies

^{1}H NMR Titration Studies. Titration of endo–exo hosts **2** or **4** with *p*-nitrophenol (PNP) in $CDCl_3$ results in a dramatic upfield shift in the ^{1}H NMR signal corresponding to the protons ortho to the exo phosphoryl (Figure 9).[1] A selective population transfer (SPT) study confirmed that the meta proton signals which shifted upfield the most upon complexation correspond to the protons meta to P_{exo}. The signal for the protons ortho to P_{exo} shift the most for every guest studied. Therefore, we used these signals to

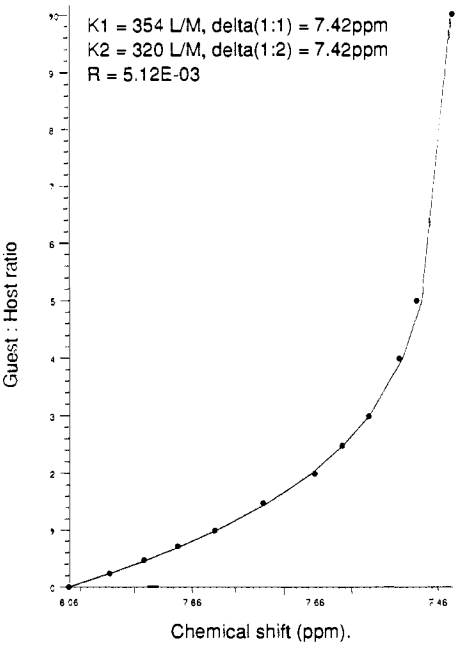

Figure 10. Plot of the chemical shift of the proton ortho to P_{exo} on **2** versus the equivalents of PNP added at 25 °C in $CDCl_3$. The points are the observed chemical shifts, and the curve is generated by the Simplex algorithm, assuming 1:2 complexation, by using the association constants and chemical shifts shown.

determine association constants. Similar treatment of exo–exo hosts **1** or **3** results in no substantial movement (NSM) of any host proton signal.[21] We deduced that exo–exo hosts **1** and **3** either did not form complexes with PNP, or they complex such that no chemical shift change of host ^{1}H NMR signals occurs upon complexation. To test which of these conclusions was correct, we prepared solutions of **2** (0.006 M) and PNP (0.012 M) in $CDCL_3$. The ^{1}H NMR spectra for these solutions were recorded, and addition of exo–exo hosts **1** or **3** was performed. The ^{1}H NMR spectrum of the resulting solution was recorded. In both cases, movement of the signals of the protons ortho to P_{exo} (**2**) in the direction toward the free host (8.06 ppm) transpired. This served as evidence that hosts **1** and **3** formed complexes with PNP, but that complexation results in no shift of host ^{1}H NMR signals. This discovery proved important in determining the preferred mechanism of 1:2 complexation in hosts **2** and **4** with PNP (Scheme II). The exo phosphoryl complexation sites in endo–exo hosts **2** and **4** are proposed to bind analogously to those in **1** and **3**. Therefore, little or no movement of host proton signals should occur upon exo complexation. We concluded that signal movement upon addition of guests in **2** and **4** was a consequence of endo complexation. Presumably, the endo complexation of PNP results in the shielding of the protons ortho to P_{exo}. Hence, the upfield shift upon addition of guests is observed. CPK models of the endo PNP complexes with **2** and **4** reveal that the aromatic ring of the guest is closer to the aromatic rings attached to the exo phosphoryl than to those attached to the endo phosphoryl.

The non-sigmoidal curve generated assuming 1:2 complexation (Figure 10) for titration of **2** with PNP is evidence for the initial endo complexation of PNP, since the calculated chemical shift of the 1:1 complex (7.42 ppm) is significantly different than the chemical shift of the free host (8.06 ppm), but identical with that of the calculated chemical shift of the 1:2 complex (7.42 ppm). However, the unmistakable sigmoidality in the Simplex-generated curve from the titration of **4** with PNP (Figure 11) provides evidence that initial exo complexation is the primary mechanism for 2:1 complexation, since the calculated chemical shift of the

(21) No substantial movement (NSM) indicates that less than 0.05 ppm shifting of any host proton occurred in the ^{1}H NMR on addition of 4 equiv of guest.

(22) O'Krongly, D. A. Ph.D. Thesis, Columbia University, 1985, pp 202–205.

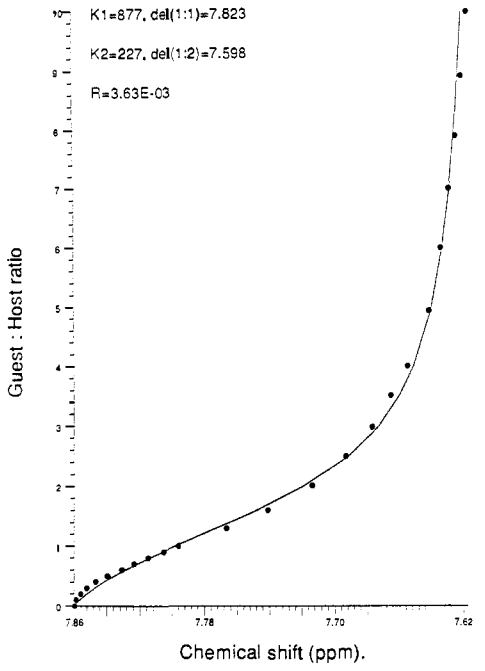

Figure 11. Plot of the chemical shift of the proton ortho to P_{exo} on **4** versus the equivalents of PNP added at 25 °C in $CDCl_3$. The points are the observed chemical shifts, and the curve is generated by the Simplex algorithm, assuming 1:2 complexation, by using the association constants and chemical shifts shown.

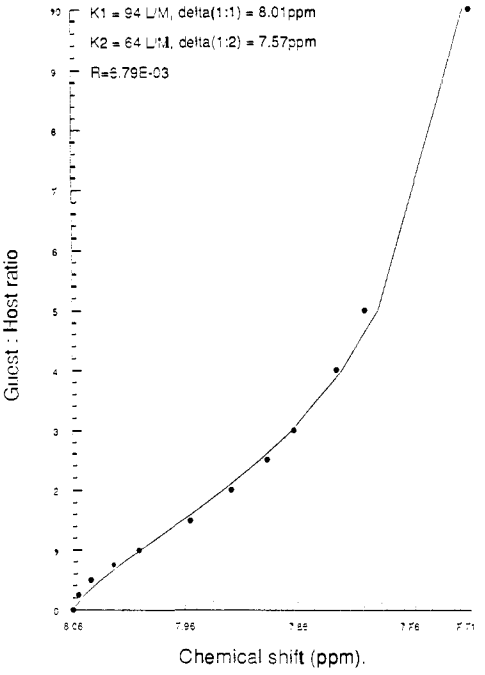

Figure 12. Plot of the chemical shift of the proton ortho to P_{exo} on **2** versus the equivalents of pentafluorophenol added at 25 °C in $CDCl_3$. The points are the observed chemical shifts, and the curve is generated by the Simplex algorithm, assuming 1:2 complexation, by using the association constants and chemical shifts shown.

Table III. Data Calculated from the Titration of **2** and **4** with Various Guests in $CDCl_3$ at 25 °C by Using ^1H NMR

	hosts			
	2		**4**	
guests	K_1, K_2,[a] M^{-1}	δ_1, δ_2,[b] ppm	K_1, K_2,[a] M^{-1}	δ_1, δ_2,[b] ppm
phenol	18_i, 1_o	7.10, 7.10		
4-cyanophenol	115_i, 486_o	7.41, 7.37	705_o, 86_i	7.85, 7.56
4-nitrophenol	354_i, 320_o	7.42, 7.42	877_o, 227_i	7.82, 7.60
2,4-dinitrophenol	NSM[c]	NSM[c]	NSM[c]	NSM[c]
4-(trifluoromethyl)-phenol	344_i, 88_o	7.59, 7.35	223_o, 64_i	7.83, 7.62
4-fluorophenol	59_i, 15_o	7.36, 7.36	25_o, 24_i	7.76, 7.60
3,4-difluorophenol	278_i, 71_o	7.69, 7.38	184_o, 47_i	7.82, 7.58
pentafluorophenol	94_o, 64_i	8.01, 7.57	270_o, 69_i	7.81, 7.57
4-[(p-nitrophenyl)-azo]phenol	218_i, 206_o	7.42, 7.46	305_o, 78_i	7.87, 7.62
6-nitro-2-naphthol	163_i, 313_o	7.44, 7.38	443_o, 113_i	7.89, 7.69
4-nitrothiophenol	NSM[c]	NSM[c]	NSM[c]	NSM[c]
benzoic acid	NSM[c]	NSM[c]	NSM[c]	NSM[c]
pyridine hydrochloride	NSM[c]	NSM[c]	NSM[c]	NSM[c]

[a] The association constants are calculated by Simplex with use of a 2:1 complexation assumption. K_1 refers to the association constant for 1:1 formation, while K_2 refers to the association constant for the formation of the 2:1 complex from the 1:1 complex. The subscripts i and o refer to endo and exo complexation, respectively. [b] δ_1 refers to the calculated chemical shift of the 1:1 complex for the proton ortho to the P_{exo}, while δ_2 refers to the calculated chemical shift of the same proton in the 2:1 complex. These are calculated by using Simplex. The ^1H chemical shifts for the proton ortho to P_{exo} for **2** and **4** respectively, are 8.06 ppm and 7.86 ppm. [c] NSM means that no substantial movement of any host proton signal (<0.05 ppm) occurred upon addition of 4 equiv of guest.

1:1 complex (7.82 ppm) is close to that of the free host (7.86 ppm), but significantly different from that of the 1:2 complex (7.60 ppm). Results from the titration of **2** and **4** with a variety of substituted phenols, 4-nitrophenol, benzoic acid, and pyridine hydrochloride using ^1H NMR are given in Table III.

Inspection of Table III provides insight into the nature of complexation in endo–exo macrocycles **2** and **4**. The association constants for formation of the 1:1 complex (K_1) range from 18 M^{-1} (phenol) to 354 M^{-1} (4-nitrophenol) for complexation of **2** with mono- or unsubstituted phenols, while the association constants for the formation of the 1:2 complexes (K_2) range from 1 M^{-1} (phenol) to 320 M^{-1} (PNP). While these values are not remarkable in our group,[9] they do illustrate the potential of phosphine oxides as loci for complexation of neutral guests in host–guest chemistry. As described for PNP, the calculated chemical shifts for the 1:1 (δ_1) and 1:2 (δ_2) complexes provide pertinent information regarding the favored route in 1:2 adduct formation. We believed that by suitably substituting the phenol we could shift the major pathway for complexation in **2** from initial endo complexation to initial exo complexation since large substituents should hinder endo complexation. Titration with 2,4-dinitrophenol results in no substantial movement (NSM) for any host proton signal. This provided evidence against any endo complexation presumably due to steric hindrance by the ortho nitro substituent. Exo complexation could not be ruled out by using ^1H NMR since exo complexation is expected to give this result. The two larger guests 4-[(*p*-nitrophenyl)azo]phenol (δ_1 = 7.42 ppm, δ_2 = 7.46 ppm) and 6-nitro-2-naphthol (δ_1 = 7.44 ppm, δ_2 = 7.38 ppm) gave surprising results, indicating that initial endo complexation was still the preferred mechanism. Titration with pentafluorophenol, however, resulted in a sigmoidal curve (δ_1 = 8.01 ppm, δ_2 = 7.57 ppm), revealing that this species prefers to complex with **2**, utilizing the initial exo pathway (Figure 12). Titration of **2** and **4** with 4-nitrothiophenol, benzoic acid, and pyridine hydrochloride resulted in NSM of host signals, indicating that no endo complexation occurs with these guests.

Titration of **4** with every guest studied resulted in either NSM of any host proton signal, or indicated complexation via the preferred initial exo complexation route. K_1 values ranged from 25 M^{-1} (4-fluorophenol) to 877 M^{-1} (PNP) for those guests effecting chemical shift movement. K_2 values ranged from 24 M^{-1} (4-fluorophenol) to 227 M^{-1} (PNP), and δ_1 values ranged from 7.76 ppm (4-fluorophenol) to 7.89 ppm (6-nitro-2-naphthol). These values are all similar to the chemical shift of free **4** (7.86 ppm), but significantly different from the δ_2 values which ranged from 7.56 ppm (4-cyanophenol) to 7.69 ppm (6-nitro-2-naphthol). All the species which effected movement of the ^1H NMR signals of **4** resulted in sigmoidal curves predicted by the initial study with PNP.[1] Titration of **2** and **4** with these guests provided additional evidence concerning our conclusions previously forwarded.[1]

Table IV. Experimental Data Determined from the Titration of **8**, **1**, and **3** with Various Guests in $CDCl_3$ at 25 °C with Use of ^{31}P NMR and PPh_3 in THF as an External Reference (δ = −6.00 ppm)

	phosphine oxide hosts					
	8		**1**		**3**	
guests	K_1,[a] M^{-1}	δ_1,[b] ppm	K_1,[c] M^{-1}	δ_1,[d] ppm	K_1,[c] M^{-1}	δ_1,[d] ppm
4-nitrophenol	299	31.94	159	32.17	102	33.26
4-cyanophenol	-	-	120	31.87	95	32.72
pentafluorophenol	-	-	63	32.92	74	33.58

[a] The association constant was calculated by using Simplex, assuming 1:1 complexation. [b] The ^{31}P chemical shift of the 1:1 complex calculated by Simplex. The ^{31}P chemical shift of **8** is 27.50 ppm. [c] The association constant was calculated by multiplying the host concentration by 2 and then using Simplex, assuming 1:1 complexation. [d] The ^{31}P chemical shift of the complexed phosphoryl P was calculated by using Simplex. The ^{31}P chemical shifts for **1** and **3**, respectively, are 27.31 ppm and 27.46 ppm.

However, we communicated that the reduction of intracavity space in **4** with respect to **2** accounted for the difference in 2:1 complexation mechanism.[1] This is doubtful upon comparison of the X-ray structural data obtained for **4** with that recently obtained for **2**. The O_{endo}–P_{exo} distance in **4** (4.68 Å) is larger than in **2** (4.20 Å). The differences in complexation mechanism are likely due to the changes in the host cavities resulting from the more helical nature of **2**.

^{31}P NMR Titration Studies. A major disadvantage of employing ^1H NMR in determining association constants in macrocycles **1–4** is that evidence of exo binding is only observed due to its competition with endo binding and not for its effect upon the chemical shift of host protons. Therefore, we utilized ^{31}P NMR to determine association constants for the two exo–exo hosts (**1** and **3**) and **8** and for confirming observations obtained by using ^1H NMR for the endo–exo hosts **2** and **4**. In contrast with the ^1H NMR upfield shift of signals upon endo complexation, all movement of ^{31}P NMR signals was downfield upon complexation. The titration studies and successful assignment of ^{31}P peaks in **8**, **2**, and **4** using Ph_2SnCl_2 as a shift reagent have already been discussed.

Results from the ^{31}P NMR titration studies of precyclophane **8** and exo–exo hosts **1** and **3** with various guests in $CDCl_3$ at 25 °C are given in Table IV. Few titration studies were performed on these phosphine oxides since we were primarily interested in intracavity adduct formation. However, these do serve as good models for comparison since only one type of phosphoryl site is present simplifying analysis. Titration of **8** with PNP yielded a K_1 of 299 M^{-1} and δ_1 of 31.94 ppm, assuming 1:1 complexation.[19] Analysis of **1** and **3** was carried out with the assumption that the phosphine oxide binding sites are not only identical, but also noninteracting. Thus, the concentration of the hosts was multiplied by two to give the effective concentration of phosphine oxide binding site. The data resulting from the titration studies was fit with use of a nonlinear least-squares curve-fitting program, assuming 1:1 complexation.[19] Adequate fitting of the data was realized in this manner. Titration of **1** was accomplished with PNP (K_1 = 159 M^{-1}, δ_1 = 32.17 ppm), 4-cyanophenol (K_1 = 120 M^{-1}, δ_1 = 31.87 ppm), and pentafluorophenol (K_1 = 63 M^{-1}, δ_1 = 32.92 ppm). Similar titrations were carried out on **3** with PNP (K_1 = 102 M^{-1}, δ_1 = 33.26 ppm), 4-cyanophenol (K_1 = 95 M^{-1}, δ_1 = 32.72 ppm), and pentafluorophenol (K_1 = 74 M^{-1}, δ_1 = 33.58 ppm). We have, therefore, obtained conclusive evidence for the exo complexation in **1** and **3**.

The results from the titration studies of **2** and **4** with several guests in $CDCL_3$ at 25 °C are presented in Table V. We hypothesized that P_{exo} should shift not only upon exo complexation, but also upon endo complexation since the ^1H NMR signals for protons ortho to P_{exo} shifted upon endo complexation. Therefore, the K_1, K_2, δ_1, and δ_2 values were calculated by analysis of P_{endo} signal movement. The K_1 and K_2 values correspond more closely with those obtained by using ^1H NMR when they are calculated with use of P_{endo} rather than P_{exo}. One exception to this was the titration with Ph_2SnCl_2 where only exo complexation was observed. Calculation using P_{exo} was employed here since endo complexation does not occur, and hence interfere with P_{exo} movement. Titration of **2** with various guests gave the following results: 4-cyanophenol (K_1 = 443 M^{-1}, K_2 = 115 M^{-1}, δ_1 = 31.21 ppm, δ_2 = 35.19 ppm), PNP (K_1 = 365 M^{-1}, K_2 = 374 M^{-1}, δ_1 = 30.44 ppm, δ_2 = 34.35 ppm), and 4-(trifluoromethyl)phenol (K_1 = 201 M^{-1}, K_2 = 51 M^{-1}, δ_1 = 31.91 ppm, δ_2 = 35.76 ppm). With all these species δ_1 is significantly different than the chemical shift of the P_{endo} signal in free **2** (25.09 ppm), indicating initial endo complexation. However, δ_2 is different than δ_1, indicating movement of P_{endo} signals upon exo complexation. No sigmoidal titration curves are observed for these species. Titration of **2** with pentafluorophenol (K_1 = 166 M^{-1}, K_2 = 42 M^{-1}, δ_1 = 26.07 ppm, δ_2 = 33.01 ppm),

Table V. Experimental Data Determined from the Titration of **2** and **4** with Various Guests in $CDCl_3$ at 25 °C using ^{31}P NMR

	phosphine oxide			
	2		**4**	
guest	K_1, K_2,[a] M^{-1}	δ_1, δ_2,[b] ppm	K_1, K_2,[a] M^{-1}	δ_1, δ_2,[b] ppm
4-cyanophenol	443_i, 115_o	31.21, 35.19	487_o, 125_i	25.94, 30.62
4-nitrophenol	365_i, 374_o	30.44, 34.35	968_o, 261_i	25.77, 30.82
4-(trifluoromethyl)-phenol	201_i, 51_o	31.91, 35.76	216_o, 55_i	25.82, 30.40
pentafluorophenol	166_o, 42_i	25.83, 33.01	355_o, 91_i	25.79, 30.48
2,6-dimethyl-4-nitrophenol	251_o, 6_i	26.07, 36.96	489_o, 5_i	25.12, 31.50
acetic acid	377_o, 2_i	25.58, 37.18	-	-

[a] The association constants are calculated by following P_{endo} ^{31}P NMR shifts by using Simplex, assuming 2:1 complexation. The subscripts i and o refer to endo and exo complexation, respectively. [b] The calculated ^{31}P chemical shifts of P_{endo} for the 1:1 (δ_1) and 2:1 (δ_2) complexes using Simplex, assuming 2:1 complexation. The chemical shifts of P_{endo} in **2** and **4** are 25.09 ppm and 24.81 ppm, respectively (PPh_3/THF = −6.00 ppm).

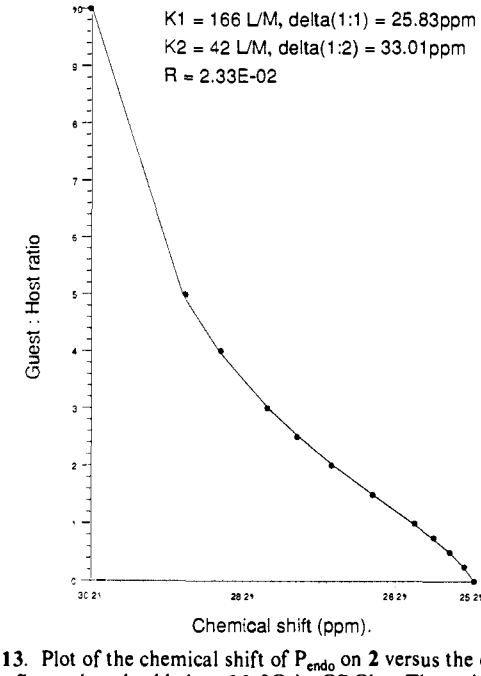

Figure 13. Plot of the chemical shift of P_{endo} on **2** versus the equivalents of pentafluorophenol added at 25 °C in $CDCl_3$. The points are the observed chemical shifts, and the curve is generated by the Simplex algorithm, assuming 1:2 complexation, by using the association constants and chemical shifts shown.

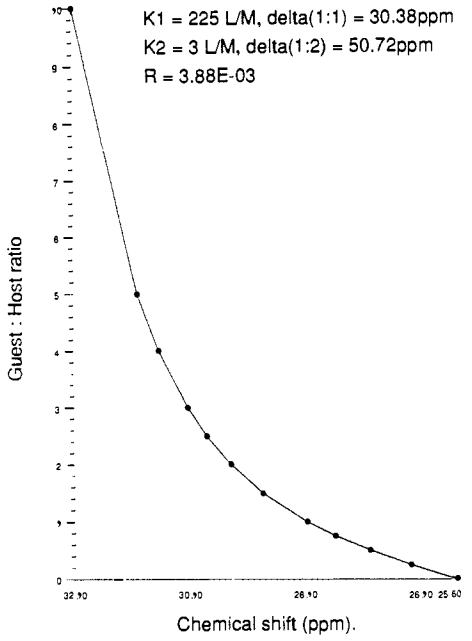

Figure 14. Plot of the chemical shift of P_{exo} on **2** versus the equivalents of pentafluorophenol added at 25 °C in $CDCl_3$. The points are the observed chemical shifts, and the curve is generated by the Simplex algorithm, assuming 1:2 complexation, by using the association constants and chemical shifts shown.

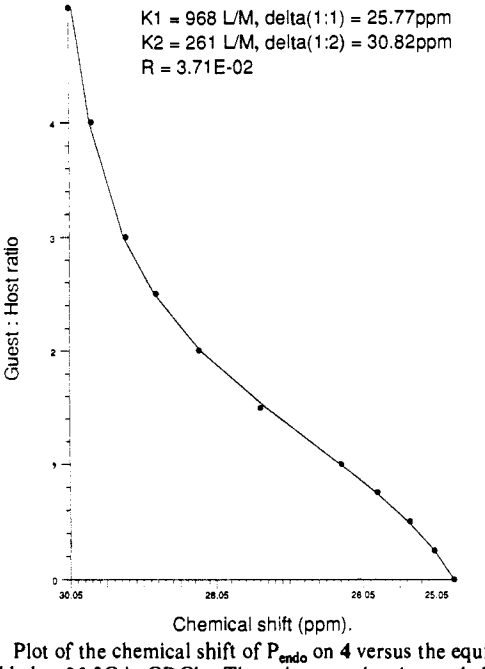

Figure 15. Plot of the chemical shift of P_{endo} on **4** versus the equivalents of PNP added at 25 °C in $CDCl_3$. The points are the observed chemical shifts, and the curve is generated by the Simplex algorithm, assuming 1:2 complexation, by using the association constants and chemical shifts shown.

the sterically encumbered 2,6-dimethyl-4-nitrophenol (K_1 = 251 M^{-1}, K_2 = 6 M^{-1}, δ_1 = 26.07 ppm, δ_2 = 36.96 ppm), and acetic acid (K_1 = 377 M^{-1}, K_2 = 2 M^{-1}, δ_1 = 25.58 ppm, δ_2 = 37.18 ppm) gave very different results. δ_1's using these species are much closer to the chemical shift of the free host P_{endo}, indicating initial exo complexation. Indeed, the curve generated with use of the Simplex algorithm following P_{endo} for titration of **2** with pentafluorophenol is clearly sigmoidal (Figure 13) while the curve following P_{exo} is obviously not (Figure 14), providing additional evidence for the conclusions drawn from the complexation of **2** with pentafluorophenol by using ^1H NMR.[19]

The data obtained from titration of endo–exo hydrogenated macrocycle **4** using ^{31}P NMR was qualitatively in good agreement with that from ^1H NMR. The K_1 values extended from 968 M^{-1} (PNP) to 216 M^{-1} (4-(trifluoromethyl)phenol) while the K_2's spanned from 261 M^{-1} (PNP) to 5 M^{-1} (2,6-dimethyl-4-nitrophenol) for those guests forming intracavity adducts. The δ_1'ss were relatively similar to the chemical shift of the free P_{endo} signal for **4** (24.81 ppm) extending from 25.94 ppm (4-cyanophenol) to 25.12 ppm (2,6-dimethyl-4-nitrophenol) while the δ_2's were remarkably dissimilar from those of free **4** ranging from 31.50 ppm (2,6-dimethyl-4-nitrophenol) to 30.40 ppm (4-(trifluoromethyl)phenol). The curves fitting the data for P_{endo} were all sigmoidal as anticipated from our ^1H NMR studies. The curves generated by following P_{exo} were all non-sigmoidal, giving further evidence for the initial exo complexation mechanism. Figures 15 and 16 are the curves generated from titration of **4** with PNP following the P_{endo} and P_{exo} signals.

Anomalous Behavior in 4. Upon examination of the data in Tables I, III, IV, and V, an anomaly in exo association constants (K_{exo}'s) in titrations employing Ph_2SnCl_2 and PNP as guests was observed. We initially became aware of this during ^{31}P NMR signal assignment. The K_{exo}'s for complexation of **8**, **2**, and **4** with Ph_2SnCl_2 are listed as follows: **8** (138 M^{-1}), **2** (243 M^{-1}), **4** (732 M^{-1}). The K_{exo} for **4** with PNP is greater than three times that for either precyclophane **8** or endo–exo diyne **2**. After rechecking these values, we hypothesized that this results from either the electronic differences between acetylenic and saturated bridges, or from transannular interaction between O_{endo} and P_{exo}. The K_{exo}'s for titration of **1**-**4**, and **8** with PNP are listed as follows: **1** (159 M^{-1} (^{31}P)); **2** (320 M^{-1} (^1H), 374 M^{-1} (^{31}P)); **3** (102 M^{-1} (^{13}P)); **4** (877 M^{-1} (^1H), 968 M^{-1} (^{31}P)); **8** (299 M^{-1} (^{31}P)). The two saturated bridge species (**3** and **4**) would be predicted to have

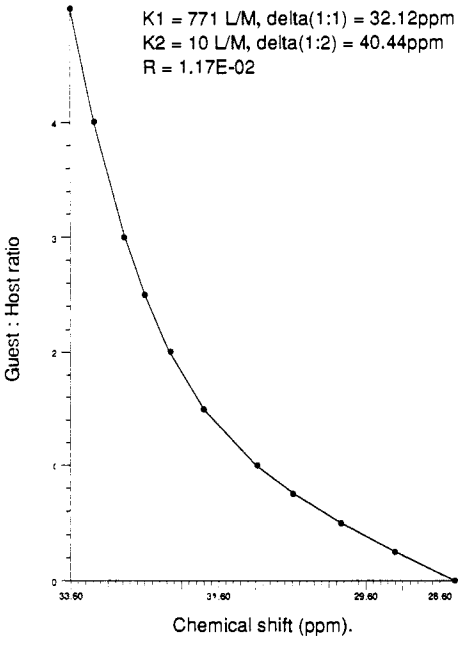

Figure 16. Plot of the chemical shift of P_{exo} on **4** versus the equivalents of PNP added at 25 °C in $CDCl_3$. The points are the observed chemical shifts, and the curve is generated by the Simplex algorithm, assuming 1:2 complexation, by using the association constants and chemical shifts shown.

larger K_{exo}'s than those for **1**, **2**, and **8** if the difference were due to the electronic effects produced on hydrogenation. Yet, not only does **3** bind PNP substantially less than **4**, it also does not bind PNP as tightly as doe **1**, **2**, or **8**. Therefore, we obtained an X-ray structure of the 1:1 complex of **4** with Ph_2SnCl_2 to document the O_{endo}–P_{exo} interaction we hypothesized. Triclinic crystals suitable for X-ray analysis were obtained from chloroform by diffusing pentane into the system. The crystal structure (Figure 17) clearly demonstrates the 1:1 and exo nature of the complex. The two phenyl substituents on the tin atom are equatorial, one chlorine is equatorial (Sn–Cl = 2.36 Å) while the other is axial (Sn–Cl = 2.44 Å), and the exo oxygen is axial (Sn–O = 2.26 Å). However, the O_{endo}–P_{exo} distance (4.70 Å) is about the same as

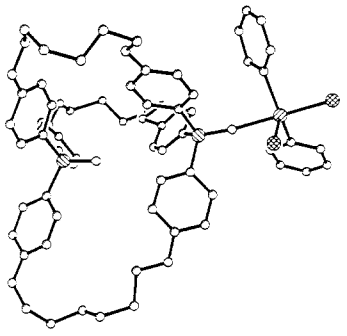

Figure 17. Representation of the 1:1 complex of endo–exo saturated bridge macrocycle **4** with Ph_2SnCl_2 generated by SHELXTL PLUS, based on X-ray data collected at −100 °C. No solvent was present in the crystal. Disorder in one of the three bridges required modeling during refinement. One of the modeled bridges is used to generate this structure. The final *R* value after refinement was 0.092. The O_{endo}–P_{exo} distance is 4.70 Å, and the Sn–O_{exo} bond length is 2.26 Å.

that in the free host (4.68 Å), and P_{exo} is clearly tetracoordinate and not pentacoordinate as we had anticipated. We are thus unable to explain the anomalous behavior of **4**.

Conclusion

The synthesis of four phosphine oxide bifunctional macrocycles containing three-dimensional cavities has been presented. In addition, the X-ray crystal structure of **1**, **2**, and **4** are reported. A simple method involving titration studies with Ph_2SnCl_2 in conjunction with 2D correlation NMR experiments allowed irrefutable assignment of the aromatic ^1H NMR signals and the ^{31}P NMR signals in endo–exo species **2** and **4**.

We recently reported the titration studies utilizing ^1H NMR for **2** and **4** with PNP.[1] We have utilized this instrumental technique for analyzing the mechanism of 1:2 complexation of hosts **2** and **4** with a variety of guests. These studies have indicated that the mechanism for 1:2 complex fomration in **2** usually favors initial endo complexation with the notable exception of pentafluorophenol. It has also been demonstrated that **4** forms 1:2 complexes with phenols preferring intial exo complexation.

^{31}P NMR allowed us to obtain mechanistic information about the 2:1 complexation which occurs in hosts **2** and **4**. This technique was employed to monitor titration of the precyclophane **8** and the exo–exo hosts (**1** and **3**), and we calculated association constants for these macrocyclic species. Use of this method provided evidence supporting the conclusions made from the ^1H NMR data. We found evidence supporting the initial endo complexation of **2** with most guests in 2:1 complex formation. However, initial exo complexation was observed with 2,6-dimethyl-4-nitrophenol, acetic acid, and pentafluorophenol, and we found that only the exo complex is formed with Ph_2SnCl_2. Complexation of **4** with guests occurred via the initial exo pathway.

The anomalously high exo association constants of **4** with PNP and Ph_2SnCl_2 relative to that in hosts **1–3** and **8** has been noted and discussed. The X-ray crystal structure of the 1:1 complex of **4** with Ph_2SnCl_2 is reported as evidence against an O_{endo}–P_{exo} interaction upon exo complexation in this cryptand.

Experimental Section

Instrumentation. Melting points were measured on a Fisher-Johns hot stage instrument and are uncorrected. ^1H NMR spectra were recorded on a Bruker WP-200 spectrometer (200.13 MHz) with TMS (δ = 0.00 ppm) as a reference, the proton decoupled ^{13}C NMR spectra were recorded on a Bruker WP-270 spectrometer (68 MHz) with $CDCl_3$ (δ = 77.0 ppm) or d_6-acetone (δ = 29.8 ppm) as references, and the proton decoupled ^{31}P NMR spectra were recorded on a Bruker WP-270 spectrometer (109 MHz) with triphenyl phosphine in THF as an external reference (δ = −6.00 ppm). The structures of the macrocycles present the scheme for numbering carbons that we used to make assignment of ^1H NMR and ^{13}C NMR signals more simple. The ^{31}P–^1H 2D correlation NMR spectra were recorded on a Bruker AM-500 spectrometer with $CDCl_3$ as a solvent and with use of the recorded chemical shifts from the separate ^1H and ^{31}P NMR spectra for **2** and **4** as references. Mass spectral data (MS) was obtained by using either a Kratos MS-25 or MS-80 spectrometer. Fast atom bombardment spectra (FAB) were collected by utilizing a Kratos MS-50TC ultrahigh resolution spectrometer. Xenon was used as the bombardment gas.

Materials. Organic chemicals used were reagent grade. Hexane and ethyl acetate were distilled in bulk prior to use. THF was distilled from sodium benzophenone ketyl. Anhydrous diethyl ether was used as obtained from sealed cans. Other solvents were used as received unless otherwise specified. Inorganic reagents were used as received. Reactions were run under nitrogen with use of flame-dried glassware.

Tris(4-methoxyphenyl)phosphine (5). The procedure of Mann and Chaplin was followed.[16] To a flame-dried 2-L flask equipped with a 500-mL dropping funnel and a West condenser was added 200 mL of freshly distilled THF and 25.2 g (1.0 mol) of magnesium turnings. *p*-Bromoanisole (5.0 mL, 40 mmol) was added. After the Grignard reaction initiated, 96.0 mL (.77 mol) of *p*-bromoanisole was added over 1 h. The flask contents was then stirred 1 h at room temperature, and subsequently 25.9 mL (.26 mol) of phosphorus trichloride was slowly injected into the stirred mixture. The reaction mixture was stirred 1 h and then poured into a mixture of 100 g of ice and 1 L of 10% HCl. Extraction was carried out with diethyl ether (3 × L). Filtration and solvent removal followed by recrystallization from ethanol yielded 51.3 g (56%) of the phosphine as white plates: mp 129–130 °C (reported mp 130–131 °C);[16] ^1H NMR (200 MHz, $CDCl_3$, TMS) δ 7.2 (dd, $^3J_{HH}$ = 9 Hz, $^3J_{PH}$ = 7 Hz, 6 H, C(2)H), 6.8 (dd, $^3J_{HH}$ = 9 Hz, $^4J_{PH}$ = 1 Hz, 6 H, C(3)H), 3.79 (s, 9 H, OCH_3); MS calculated for $C_{21}H_{21}O_3P$ 352.1229, found 352.1243.

Tris(4-methoxyphenyl)phosphine Oxide (6). To a stirred suspension of 7.7 g (22 mmol) of tris(4-methoxyphenyl)phosphine (**5**) in 250 mL of water was added 3.7 g (23 mmol) of potassium permanganate. The reaction was stirred at room temperature for 16 h and poured into 1 L of water. Extraction was carried out with use of chloroform (3 × 600 mL). The combined organic layers were washed with water (3 × 500 mL) and then dried over magnesium sulfate. Filtration followed by solvent removal yielded 7.3 g (90%) of the crude product. Recrystallization from cyclohexane afforded 7.0 g (86%) of the phosphine oxide as white needles: mp 145–146 °C (reported mp 143–144 °C);[17] ^1H NMR (200 MHz, CD_3COCD_3, TMS) δ 7.5 (dd, $^3J_{PH}$ = 11.5 Hz, $^3J_{HH}$ = 9 Hz, 6 H, C(2)H), 7.0 (dd, $^3J_{HH}$ = 9 Hz, $^4J_{PH}$ = 2.5 Hz, 6 H, C(3)H), 3.86 (s, 9 H, OCH_3); ^{13}C NMR (68 MHz, $CDCl_3$, $CDCl_3$) δ 162.11 (s, C(4)), 133.64 (d, $^2J_{PC}$ = 11.2 Hz, C(2)), 124.37 (d, $^1J_{PC}$ = 110.9 Hz, C(1)), 113.76 (d, $^3J_{PC}$ = 13.1 Hz, C(3)), 55.12 (s, OCH_3); ^{31}P NMR (109 MHz, $CDCl_3$, PPh_3/THF) δ 27.76 (s, P); MS calculated for $C_{21}H_{21}O_4P$ 368.1178, found 368.1175.

Tris(4-hydroxyphenyl)phosphine Oxide (7). Into a 2-L flask equipped with a West condenser were placed 51.3 g (139 mmol) of tris(4-methoxyphenyl)phosphine oxide (**6**) and methylene chloride (1 L). The stirred mixture was cooled to −78 °C by immersion in an acetone/dry ice bath, and boron tribromide (200 g, 798 mmol) was injected. The reaction mixture was warmed to room temperature, stirred for 24 h, and poured into cold water (2 L). The flask was heated while stirring until all organic solvent was removed and then cooled to room temperature. Filtration was performed and the filtrate extracted with ethyl acetate (2 × 1 L). The collected solid was added to the combined organic layers and recrystallized, yielding 44.1 g (97%) of the deprotected phosphine oxide as white needles: mp 263–264 °C (reported mp 273-275 °C);[17] ^1H NMR (200 MHz, CD_3COCD_3, TMS) δ 9.8 (s, br, 3 H, OH), 7.5 (dd, $^3J_{PH}$ = 11.5 Hz, $^3J_{HH}$ = 9 Hz, 6 H, C(2)H), 7.0 (dd, $^3H_{HH}$ = 9 Hz, $^4J_{PH}$ = 2.5 Hz, 6 H, C(3)H); ^{13}C NMR (68 MHz, CD_3COCD_3, CD_3COCD_3) δ 161.92 (s, C(4)), 134.61 (d, $^2H_{PC}$ = 11.2 Hz, C(2)), 123.15 (d, $^1J_{PC}$ = 112.8 Hz, C(1)), 116.41 (d, $^3J_{PC}$ = 13.1 Hz, C(3)); ^{31}P NMR (109 MHz, CD_3COCD_3, PPh_3/THF) δ 29.72 (s, P); MS calculated for $C_{18}H_{15}O_4P$ 326.0708, found 326.0702.

Tris[4-(propargyloxy)phenyl]phosphine Oxide (8). To a 500-mL flask containing 250 mL of acetone, 7.2 g (22 mmol) of tris(4-hydroxyphenyl)phosphine oxide (**7**), and 25.0 g (181 mmol) of K_2CO_3 was added 15.0 mL (199 mmol) of propargyl bromide. The stirred mixture was refluxed for 9 h, transferred to a separatory funnel containing 1 L of water, and extracted with chloroform (3 × 600 mL). Drying of the organic layers over anhydrous $MgSO_4$ followed by filtration and solvent removal afforded 8.6 g of the crude product. Recrystallization from a 50/50 ethanol/water mixture gave 7.6 g (78%) of the phosphine oxide as white needles: mp 130–132 °C; ^1H NMR (200 MHz, $CDCl_3$, TMS) δ 7.6 (dd, $^3J_{PH}$ = 11.5 Hz, $^3J_{HH}$ = 9 Hz, 6 H, C(2)H), 7.0 (dd, $^3J_{HH}$ = 9 Hz, $^4J_{PH}$ = 2.5 Hz, 6 H, C(3)H), 4.7 (d, $^4J_{HH}$ = 2.5 Hz, 6 H, OCH_2), 2.5 (t, $^4J_{HH}$ = 2.5 Hz, 3 H, OCH_2CCH); ^{13}C NMR (68 MHz, $CDCl_3$, $CDCl_3$) 160.05 (s, C(4)), 133.63 (d, $^2J_{PC}$ = 11.2 Hz, C(2)), 125.08 (d, $^1J_{PC}$ = 110.3 Hz, C(1)), 114.65 (d, $^3J_{PC}$ = 13.0 Hz, C(3)), 77.66 (s, OCH_2CCH), 76.10 (s, OCH_2CCH), 55.57 (s, OCH_2CCH); ^{31}P NMR (109 MHz, $CDCl_3$, PPh_3/THF) δ 27.50 (s, P); MS calculated for $C_{27}H_{21}O_4P$ 440.1178, found 440.1179.

Exo(P=O)-Exo(P=O) and Endo(P=O)-exo(P=O) Phosphine Oxide Hosts (1 and 2, respectively) with Diyne Bridges. A solution of 5.40 g (12.3 mmol) of tris[4-(propargyloxy)phenyl]phosphine oxide (**8**) in pyridine (1.5 L) was heated while stirring until a constant temperature of 60 °C was achieved, and 22 g (110 mmol) of $Cu(OAc)_2 \cdot H_2O$ was added. The reaction was then stirred at 60 °C for 2 h. The reaction was poured into a mixture of chloroform (2 L) and water (2 L), and concentrated hydrochloric acid was added in small portions until the pH reached 1. The layers were separated, and the organic layer was washed with an aqueous 10% hydrochloric acid solution (2 × 500 mL), with aqueous sodium bicarbonate (1 L), and then with aqueous saturated sodium chloride (1 L). The organic layer was then dried over anhydrous magnesium sulfate and filtered. Solvent removal afforded 5.32 g of crude product. Column chromatography (4 cm × 40 cm column, 11-cm silica gel, ethyl acetate) provided a 1.40 g (26%) mixture of **1** and **2**. Recrystallization from methanol with a trace of chloroform provided 745 mg (14%) of pure exo-exo host **1** in two crops as colorless needles. Column chromatography (4 cm × 40 cm column, 11-cm silica gel, ethyl acetate) performed on the mother liquors yielded 385 mg (7.2%) of the endo-exo host **2**. Recrystallization from chloroform/diethyl ether afforded 351 mg (7%) of **2** as colorless needles.

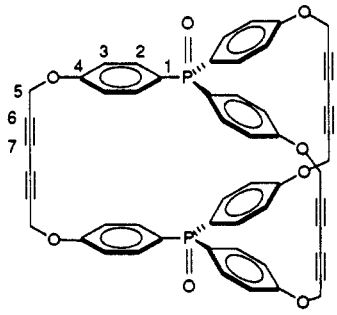

Data for **1**: mp, decomposes > 165 °C; ^{1}H NMR (200 MHz, $CDCl_3$, TMS) δ 7.67 (dd, $^3J_{PH}$ = 11.5 Hz, $^3J_{HH}$ = 9 Hz, 12 H, C(2)H), 7.07 (dd, $^3J_{HH}$ = 9 Hz, $^4J_{PH}$ = 2.5 Hz, 12 H, C(3)H), 4.85 (s, 12 H, OCH_2); ^{13}C NMR (68 MHz, 20% MeOH/$CDCl_3$, $CDCl_3$) δ 160.04 (s, C(4)), 133.57 (d, $^2J_{PC}$ = 11.4 Hz, C(2)), 123.73 (d, $^1J_{PC}$ = 111.8 Hz, C(1)), 114.70 (d, $^3J_{PC}$ = 13.2 Hz, C(3)), 73.90 (s, C(6)), 70.72 (s, C(7)), 55.24 (s, C(5)); ^{31}P NMR (109 MHz, $CDCl_3$, PPh_3/THF) δ 27.31 (s, P(1)); FAB calculated for $C_{54}H_{36}O_8P_2$ 874.1887, found 875.

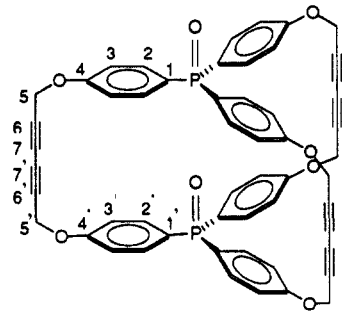

Data for **2**: mp, decomposes > 135 °C; ^{1}H NMR (200 MHz, $CDCl_3$, TMS) δ 8.06 (dd, $^3J_{PH}$ = 11.5 Hz, $^3J_{HH}$ = 9 Hz, 6 H, C(2)H), 7.63 (dd, $^3J_{PH}$ = 11.5 Hz, $^3J_{HH}$ = 9 Hz, 6 H, C(2')H), 7.08 (m, 12 H, C(3)H, C(3')H), 4.85 (s, 6 H, OCH_2), 4.73 (s, 6 H, OCH_2); ^{13}C NMR (68 MHz, $CDCl_3$, $CDCl_3$) δ 160.47 (s, C(4) or C(4')), 159.26 (s, C(4) or C(4')), 133.94 (d, $^2J_{PC}$ = 11.7 Hz, C(2) or C(2')), 133.66 (d, $^2J_{PC}$ = 11.3 Hz, C(2) or C(2')), 124.43 (d, $^1J_{PC}$ = 110.6 Hz, C(1) and C(1')), 116.48 (d, $^3J_{PC}$ = 13.1 Hz, C(3) or C(3')), 114.97 (d, $^3J_{PC}$ = 13.2 Hz, C(3) or C(3')), 75.55 (s, C(6) or C(6')), 74.51 (s, C(6) or C(6')), 73.23 (s, C(7) or C(7')), 70.61 (s, C(7) or C(7')), 56.23 (s, C(5) or C(5')), 56.10 (s, C(5) or C(5')); ^{31}P NMR (109 MHz, $CDCl_3$, PPh_3/THF) δ 25.46 (s, P_{exo}), 25.18 (s, P_{endo}); FAB calculated for $C_{54}H_{36}O_8P_2$ 874.1887, found 875.

Exo(P=O)-Exo(P=O) Saturated Bridge Host 3. To a solution of 99.0 mg (113 μmol) of exo-exo diyne bridged host **1** in 5 mL of DMF was added 129 mg (61 μmol Pd) of 5% palladium on calcium carbonate. The mixture was shaken for 17.5 h under hydrogen (20 PSI) at room temperature. The reaction was then added to 100 mL of chloroform and filtered through a Celite pad. Solvent removal yielded 121 mg of crude product. Recrystallization from ethyl acetate afforded 48.3 mg (47%) of **3** as white crystals.

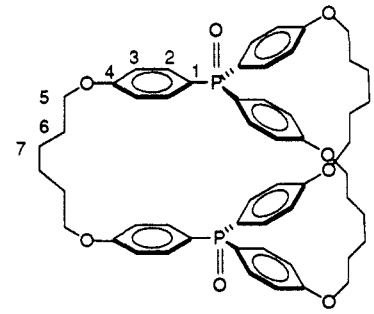

Data for **3**: mp, decomposes >287 °C; ^{1}H NMR (200 MHz, $CDCl_3$, TMS) δ 7.50 (dd, $^3J_{PH}$ = 11.5 Hz, $^3J_{HH}$ = 9 Hz, 12 H, C(2)H), 6.84 (dd, $^3J_{HH}$ = 9 Hz, $^4J_{PH}$ = 2.5 Hz, 12 H, C(3)H), 4.03 (t, $^3J_{HH}$ = 5.6 Hz, 12 H, OCH_2), 1.50-1.90 (m, 24 H, C(6)H, C(7)H); ^{13}C NMR (126 MHz, $CDCl_3$, $CDCl_3$) δ 161.72 (s, C(4)), 133.51 (d, $^2J_{PC}$ = 11.0 Hz, C(2)), 124.17 (d, $^1J_{PC}$ = 110.9 Hz, C(1)), 114.32 (d, $^3J_{PC}$ = 12.9 Hz, C(3)), 67.21 (s, C(5)), 27.66 (s, C(6)), 24.49 (s, C(7)); ^{31}P NMR (109 MHz, $CDCl_3$, PPh_3/THF) δ 27.46 (s, P); FAB calculated for $C_{54}H_{60}O_8P_2$ 898.3766, found 989.

Endo(P=O)-Exo(P=O) Saturated Bridge Host 4. To a solution of 137 mg (157 μmol) of endo-exo diyne bridged host **2** in 7 mL of DMF was added 167 mg (78 μmol Pd) of 5% palladium on calcium carbonate. The mixture was shaken at room temperature for 24 h under hydrogen (20 PSI). The reaction was then added to 100 mL of chloroform and filtered through a Celite pad. Removal of the solvent yielded 139 mg of the crude reaction product. Recrystallization from ethyl acetate yielded 75 mg (53%) of **4** as triclinic colorless crystals.

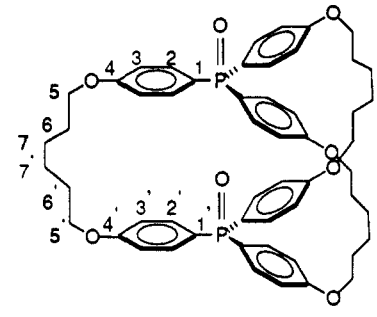

Data for **4**: mp 254-256 °C; ^{1}H NMR (200 MHz, $CDCl_3$, TMS) δ 7.86 (dd, $^3J_{PH}$ = 11.5 Hz, $^3J_{HH}$ = 9 Hz, 6 H, C(2)H, 7.51 (dd, $^3J_{PH}$ = 11.5 Hz, $^3J_{HH}$ = 9 Hz, 6 H, C(2')H), 6.94 (dd, $^3J_{HH}$ = 9 Hz, $^4J_{PH}$ = 2.5 Hz, 6 H, C(3')H), 6.81 (dd, $^3J_{HH}$ = 9 Hz, $^4J_{PH}$ = 2.5 Hz, 6 H, C(3)H), 4.21 (t, $^3J_{HH}$ = 5.9 Hz, 6 H, C(5)H or C(5')H), 3.85(t, $^3J_{HH}$ = 7.0 Hz, 6 H, C(5)H or C(5')H), 1.40-2.00 (m, 24 H, C(6)H, C(6')H, C(7)H, C(7')H); ^{13}C NMR (68 MHz, $CDCl_3$, $CDCl_3$) δ 161.83 (s, C(4) or C(4')), 161.49 (s, C(4) or C(4')), 134.61 (d, $^2J_{PC}$ = 12.3 Hz, C(2) or C(2')), 133.77 (d, $^2J_{PC}$ = 10.6 Hz, C(2) or C(2')), 125.02 (d, $^1J_{PC}$ = 110.0 Hz, C(1) or C(1')), 124.90 (d, $^1J_{PC}$ = 108.1 Hz, C(1) or C(1')), 115.18 (d, $^3J_{PC}$ = 12.5 Hz, C(3) or C(3')), 114.20 (d, $^3J_{PC}$ = 13.0 Hz, C(3) or C(3')), 67.20 (s, C(5) or C(5')), 67.47 (s, C(5) or C(5')), 28.76 (s, C(6) or C(6')), 28.41 (s, C(6) or C(6'), 24.57 (s, C(7) and C(7')); ^{31}P NMR (109 MHz, $CDCl_3$, PPh_3/THF) δ 28.40 (s, P_{exo}), 24.81 (s, P_{endo}); FAB calculated for $C_{54}H_{60}O_8P_2$ 898.3766, found 899.

Preparation of Host and Guest Solutions for Titration Studies. All titration studies were performed in $CDCl_3$ at 25 °C with $CHCl_3$ as a reference (δ = 7.26 ppm) for ^{1}H NMR studies and PPh_3 in THF as an external reference (δ = -6.00 ppm) for ^{31}P NMR studies. All guests were obtained from Aldrich and recrystallized prior to use with the exceptions of 6-nitro-2-naphthol and 4-[(*p*-nitrophenyl)azo]phenol which were prepared following known procedures.[23,24] In general, host solutions of macrocycles **1-4** were prepared with an initial concentration of 0.010 M in $CDCl_3$ while solutions of the precyclophane **8** were prepared with an initial concentration of 0.020 M. Guest titration solutions were generally prepared with a concentration of 0.10 M in $CDCl_3$. The exceptions for the ^{1}H NMR studies of **2** are listed with the initial concentration of the host followed by the concentration of the guest and the name of the guest: 0.0024 M, 0.072 M (4-nitrophenol); 0.0092 M, 0.0092 M (4-cyanophenol); 0.0075 M, 0.0050 M (6-nitro-2-naphthol); 0.0047 M, 0.0166 M

(23) Sheridan, R. E. Ph.D. Thesis, University of Wisconsin—Madison, 1988, pp 96-99.

(24) Sheridan, R. E. Ph.D. Thesis, University of Wisconsin—Madison, 1988, pp 89-90.

(4-[(p-nitrophenyl)azo]phenol); 0.0092 M, 0.092 M (phenol). The exceptions for the ^1H NMR studies of **4** are listed with use of the same format: 0.015 M, 0.094 M (4-cyanophenol); 0.0075 M, 0.075 M (4-fluorophenol); 0.010 M, 0.050 M (6-nitro-2-naphthol); 0.0075 M, 0.028 M (4-[(p-nitrophenyl)azo]phenol). For all studies, 400 μL of the host solution was used.

Acknowledgment. We gratefully acknowledge J. E. Cochran for his assistance with the ^{31}P-^1H correlation 2D NMR experiments. Acknowledgement is made for partial support of this work by the National Science Foundation and the Office of Naval Research.

Supplementary Material Available: Tables of X-ray data for **1**, **2**, **4**, and the 1:1 adduct of **4** with Ph_2SnCl_2 including crystal data, collection parameters, solution and refinement data, atomic coordinates and equivalent isotropic displacement parameters, bond lengths and angles, anisotropic displacement parameters, hydrogen atom coordinates, and isotropic displacement parameters (49 pages); tables of observed and calculated structure factors (121 pages). Ordering information is given on any current masthead page.

Reactivity of 8,11-Dihalo[5]metacyclophanes[1]

Leonardus W. Jenneskens,† Henricus J. R. de Boer, Willem H. de Wolf, and Friedrich Bickelhaupt*

Contribution from the Scheikundig Laboratorium, Vrije Universiteit, De Boelelaan 1083, 1081 HV Amsterdam, The Netherlands. *Received May 31, 1990*

Abstract: The highly bent and strained 8,11-dihalo[5]metacyclophanes **1b–d** were subjected to a variety of reactions in order to compare their behavior with that of normal, planar aromatics. Indeed, a strongly deviating reactivity of **1** was observed. With acid, rapid Wagner–Meerwein rearrangement to the ortho isomers **3** occurred, with partial loss of the substituent at position 11 (between the bridge) to furnish **4**; theoretical calculations show that relief of strain on bridgehead protonation is the initiating step. Irradiation of **1** furnished mainly **3**. This rearrangement was shown by ^{13}C-labeling to proceed via a benzvalene intermediate; a minor side reaction was radical cleavage of the 11-halogen which leads to radical attack at the central methylene group of the bridge and finally to **15**. The transformation **1** → **15** was more efficiently achieved with the complex reducing agent $NaH/Ni(OAc)_2$; in this case, however, removal of the second halogen to **18** and overreduction to **19** also occurred. Similarly, attempted catalytic reductive removal of the halogen was not successful, as the hydrogenation went on to the fully saturated bicyclo[5.3.1]undecane (**16**). The high reactivity of the aromatic nucleus was also apparent from the unusual ease of Diels–Alder reactions under rather mild conditions. Remarkable, too, is the reactivity of **1b–d** toward organolithium reagents. While *n*-butyllithium gave variable results depending on the halogen, *tert*-butyllithium showed either the unusual S_N2-substitution of Cl-11 in **1b** (to give **1e**), the expected double bromine–lithium exchange with **1c** (to give **25**), or a single-electron-transfer reaction with **1d** (to give **15d**). It is concluded that the enhanced and/or unusual reactivity of [5]metacyclophanes is mainly due to relief of strain in the initial stages of these reactions and not (primarily) to reduced aromatic character.

One of the intriguing aspects in the chemistry of short-bridged [*n*]cyclophanes is the question how bending of the benzene ring influences the chemical and physical properties of these highly strained compounds. In contrast to the [*n*]paracyclophanes, which have been studied experimentally[2,3] and theoretically,[4] the [*n*]-metacyclophanes have received less attention.

Although the synthesis of [*n*]metacyclophanes with n = 10, 7, 6,[5] and 5[6] has been reported and the intermediacy of [4]metacyclophane[7] has been invoked, experimental data concerning their reactivity are scarce. Nevertheless, it could be deduced that [*n*]metacyclophanes with $n \leq 7$ possess extraordinary properties.[2b,6b,8,9] This was initially rationalized by invoking the occurrence of bond fixation in the bent benzene ring toward a 1,3,5-cyclohexatriene-like structure.[9a]

However, when crystalline derivatives of the hitherto smallest isolable representative of [5]metacyclophane (**1a**), i.e., 8,11-dihalo[5]metacyclophanes (**1b–d**) became available (Scheme I),[10] an X-ray structure determination of 8,11-dichloro[5]metacyclophane (**1b**) unambiguously showed that despite the large deviations from planarity of the bent benzene ring (e.g., at the bow of the boat, the bending angle is 26.8°), the aromatic carbon–carbon bond lengths were practically uniform and typical for a delocalized aromatic compound (1.393 ± 0.007 Å).[11] Obviously, bond fixation cannot be responsible for the extraordinary reactivity of [*n*]metacyclophanes with $n \leq 7$. Consequently,

Scheme I[a]

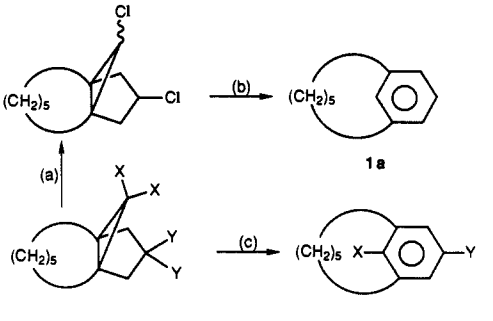

2a : X = Y = Cl **1b** : X = Y = Cl
2b : X = Y = Br **1c** : X = Y = Br
2c : X = Br, Y = Cl **1d** : X = Br, Y = Cl

[a] (a) **2a** + $2Ph_3SnH$; (b) *t*-BuOK; (c) $AgClO_4$, lutidine, THF.

an explanation was put forward based on a systematic theoretical investigation of [*n*]metacyclophanes with n = 7, 6, 5, and 4.[12a]

† Present address: AKZO Research Laboratories Arnhem, Corporate Research, P.O. Box 9300, 6800 SB Arnhem, The Netherlands.

(1) Taken in part from Jenneskens, L. W. Ph.D. Thesis, Vrije Universiteit, Amsterdam, The Netherlands, 1986.

(2) For reviews see: (a) Keehn, P. M.; Rosenfeld, S. M. *Cyclophanes*; Academic Press: New York, 1983. (b) Bickelhaupt, F.; De Wolf, W. H. *Recl. Trav. Chim. Pays-Bas* **1988**, *107*, 459. (c) Bickelhaupt, F. *Pure Appl. Chem.* **1990**, *62*, 373.

0002-7863/90/1512-8941$02.50/0